bioRxiv preprint doi: https://doi.org/10.1101/2020.07.13.198457; this version posted August 3, 2020. The copyright holder for this preprint (which was not certified by peer review) is the author/funder, who has granted bioRxiv a license to display the preprint in perpetuity. It is made available under aCC-BY-NC-ND 4.0 International license.

Transcriptional analysis of *Colletotrichum fructicola* from Different Geographic regions inoculated to *Camellia oleifera*

Shimeng Tan[1, 2, 3, 4], Yanying Chen[1, 2, 3, 5], Guoying Zhou[1, 2, 3, 4], Junang Liu[1, 2, 3, 5]*

[1] Key Laboratory of National Forestry and Grassland Administration on Control of Artificial Forest Diseases and Pests in South China, Central South University of Forestry and Technology, Changsha 410004, China;

[2] Hunan Provincial Key Laboratory for Control of Forest Diseases and Pests, Central South University of Forestry and Technology, Changsha 410004, China;

[3] Key Laboratory for Non-wood Forest Cultivation and Conservation of Ministry of Education, Central South University of Forestry and Technology, Changsha 410004, China;

[4] College of Biological Science and Technology, Central South University of Forestry and Technology, Changsha 410004, China;

[5] College of Forestry, Central South University of Forestry and Technology, Changsha 410004, China.

* Corresponding author: Junang Liu, kjc9620@163.com.

bioRxiv preprint doi: https://doi.org/10.1101/2020.07.13.198457; this version posted August 3, 2020. The copyright holder for this preprint (which was not certified by peer review) is the author/funder, who has granted bioRxiv a license to display the preprint in perpetuity. It is made available under aCC-BY-NC-ND 4.0 International license.

Abstract

Aim

The study hopes to investigate differences in molecular processes and regulatory genes at different stages of infection of *Colletotrichum fructicola*, the dominant pathogen of oil tea (*Camellia oleifera*) anthracnose in China.

Methods

The study compared the pathogenicity of *C. fructicola* from different populations (Wuzhishan, Hainan province and Shaoyang, Hunan province), and gene expression of representative strains of the two populations before and after infection with *Camellia oleifera* using RNA sequencing.

Results

We found that *C. fructicola* from Wuzhishan has a stronger ability to infect and impact *oil tea* leaf tissue. Up-regulated genes in the two geographic populations following infected to oil tea were associated with a number of ribosome-related GO and KEGG pathways, and were significantly enriched in galactosidase activity, glutamine family amino acid metabolism, arginine and proline metabolism. Up-regulated gene lists associated with infection by the Wuzhishan strains were significantly enriched in ribosome-related metabolic pathways as well as purine metabolism pathways, while Shaoyang strains were not significantly enriched in these processes.

Conclusions

These results indicate that *C. fructicola* obtained sugars and amino acids from *oil tea* tissue to resist host immune pressure. Moreover, the greater regulation of purine metabolism pathway in the Wuzhishan strain inoculated to oil tea might contribute to its stronger pathogenicity.

Key words: Anthracnose of *Camellia oleifera*, *Colletotrichum fructicola*, Transcriptome, Differential expression

Introduction

Oil tea (*Camellia oleifera*) is an agronomically and culturally important edible woody oil tree species found in China. Oil extracted from the seeds of *oil tea* is comparable to olive (*Olea europaea*) oil. *Oil tea* is widely distributed between the northern latitudes of 32°57’ and 11°17’ in China (Cui et al. 2016). Suitable climates for growth of *oil tea* are generally mild, receive sufficient sunshine and rain, and have short or no ice periods, therefore occurrence of disease and damage due to insect pests are frequent (Zhou et al. 2017). Anthracnose is a prevalent disease which affects *oil tea*, is caused by *Colletotrichum fructicola*, and is readily dispersed via spores. Spores of anthracnose can survive winter conditions and result in continuous infections year over year (Ye and He 2011).

bioRxiv preprint doi: https://doi.org/10.1101/2020.07.13.198457; this version posted August 3, 2020. The copyright holder for this preprint (which was not certified by peer review) is the author/funder, who has granted bioRxiv a license to display the preprint in perpetuity. It is made available under aCC-BY-NC-ND 4.0 International license.

Anthracnose can cause leaf fall, flower fall and fruit damage, which can impact yield or oil quality, leading to economic loss.

Colletotrichum fungus is a globally distributed and important pathogen. Colletotrichum fungus is a semi-live plant fungus, and can affect almost all crops and economic plants. The conidia colletotrichum fungus are spread by wind, rain, insects and other media. Conidia germinate in aqueous environments to form appressoriums and produce infection nails which can puncture epidermal tissues such as plant leaves and peels. After invading the host, mycelia of colletotrichum fungi are quickly formed between plant cells, destroy plant tissues and use their nutrients for further replication (Chen et al. 2009; Wang et al. 2004). To date, 8 species of anthracnose pathogens of *oil tea* have been classified based on morphological and polygenic molecular identification (Jiang and Li 2018; Li et al. 2017; Tang et al. 2015). Of identified *oil tea*, *C. fructicola* has the highest isolation rate in diseased leaf samples in China, and is the dominant pathogen of Camellia anthracnose (Li et al. 2016). Recent research on the prevention and treatment of anthracnose in oil tea has focused on application of new chemicals or biological controls such as bacteria (Deng et al. 2017; Zhou 2015). However, it has been suggested that to prevent occurrence of anthracnose in oil tea, it is necessary to have a deeper understanding of its pathogenic mechanisms to develop specific control measures. Therefore, in the current study we focused on the pathogenesis of *C. fructicola* on oil tea leaves, with the aim of improving our understanding of the molecular mechanisms of pathogenesis of *C. fructicola* infection of oil tea.

When a pathogen colonizes and infects a plant, defense responses aim to nutritional starve the fungi and subject it to reactive oxygen species (ROS) stress (Deng and Naqvi 2019). Initiation and control of plant defense responses rely on flexible and rapid molecular regulation of numerous pathways in responses to incursion by a pathogen. The infection of plants by semi-living vegetative fungi is a continuous and staged process whereby infection of plants by Colletotrichum fungi can be divided into two stages: vegetative and death phase. Hyphae growth of fungi and its spread is dependent on nutritional availability (Curry et al. 2002). Transcriptome sequencing as emerged as a useful tool for investigating the molecular regulation of different stages of infection by *C. fructicola*.

To investigate molecular mechanisms of pathogenicity of *C. fructicola* from different geographical populations, we analyzed fungi isolated from oil tea samples produced in Shaoyang, Hunan province and Wuzhishan, Hainan province, China via RNA sequencing.

Materials and methods

bioRxiv preprint doi: https://doi.org/10.1101/2020.07.13.198457; this version posted August 3, 2020. The copyright holder for this preprint (which was not certified by peer review) is the author/funder, who has granted bioRxiv a license to display the preprint in perpetuity. It is made available under aCC-BY-NC-ND 4.0 International license.

C. fructicola used for experiments was isolated from diseased oil tea leaves collected from Shaoyang, Hunan and Wuzhishan, Hainan, which were stored at -80 °C. Four strains of *C. fructicola* for test were from Shaoyang, Hunan, and 7 strains of *C. fructicola* for test were from Wuzhishan, Hainan. The geographical and climatic characteristics of the two locations are shown in Table 1 (Ma 2010; Su 2018; Zheng et al. 2016).

Media preparation

Potato dextrose agar medium (PDA medium) consisted of; 200g peeled potatoes (from local market in Changsha city, China) was added to 1000mL water and heated for 20 minutes. The mixture was filtered through gauze, and 20g glucose and 20g agar were added to the filtrate. The mixture was autoclaved at 121 °C for 20 minutes. The potato dextrose broth medium (PDB medium) can be added without agar. One gram of yeast extract was added to 1L of PDA or PDB medium to promote production of conidia.

Inoculation experiment on leaves of oil tea

The pathogenicity of the tested strains was determined *in vitro* by the injury inoculation test using leaves of the *Oil tea,* Huashuo. Young leaves were collected, petioles were sealed with paraffin wax, and then placed into a glass petri dish with wet cotton pads added to maintain humidity. A sterilized needle was used to make six pinholes along each leaf surface, three on left half and three on right half of each leaf. There would be eight leaves replicates and 48 pinholes in total. Leaves were inoculated with mycelium from Shaoyang and Wuzhishan strains, the left half with Shaoyang and right half of the leaf with Wuzhishan, each pinhole was inoculated with a 6mm diameter mycelium piece, for 24 inoculation samples per strain total.

Petri dishes were sealed with parafilm and cultured in the dark at 28 °C for 96 hours. Leaves were then removed and the diameter of the diseased spots was measured and photographed.

Sampling of RNA

Two representative strains were cultured on a PDA solid medium for 96 hours. Hyphae pieces at the edge of several colonies were cut and transferred to 100 mL of prepared PDB medium, and cultured on a shaker at 160 rpm and 28 °C for 48 hours. The culture solution was filtered through three layers of microscope wipe paper into new centrifuge tubes and then centrifuged at 5000 rpm for 3 minutes. The supernatant was poured off, spores were rinsed twice with sterile water and sterile water was added to reconstitute spores at a concentration of 1×10^9 pcs / mL. Next, 1.5mL of spore solution was placed into a 1.5mL centrifuge tube and centrifuged at 12000rpm for 2

bioRxiv preprint doi: https://doi.org/10.1101/2020.07.13.198457; this version posted August 3, 2020. The copyright holder for this preprint (which was not certified by peer review) is the author/funder, who has granted bioRxiv a license to display the preprint in perpetuity. It is made available under aCC-BY-NC-ND 4.0 International license.

min. The supernatant was removed to obtain conidia samples which were immediately frozen with liquid nitrogen and stored in a -80 °C refrigerator.

Sterile water was added to the remaining spore fluid for dilution, and the number of spores was counted to adjust the concentration of spore fluid to 1×10^6 pcs / mL. Petioles were sealed with wax and placed in a petri dish with wet absorbent cotton. The spore fluid was evenly sprayed onto the leaves, and then the petri dish was sealed. Leaves were incubated at 28 °C in the dark for 96 hours. After incubation, leaves were cut and placed into collection tubes, then immediately frozen with liquid nitrogen and transferred to a -80 ° C refrigerator. There were 3 biological replicates per sample.

RNA sequencing and data analysis

The spores and lesion samples were sent to Genedenovo Biotechnology Co., Ltd, Guangzhou, China. for RNA extraction and RNA sequencing. Among them, spore sample group number is identified as S (Start), and lesion sample group number is L (Later). Data analysis was performed online using the Omicsmart platform (Genedenovo Biotechnology Co., Ltd, Guangzhou, China; https:// www. omicsmart. com/).

Real-time PCR

The kits: FastQuant RT Kit with gDNase (TIANGEN Biotech Co., Ltd, Beijing, China); SuperReal PreMix Plus (SYBR Green) (TIANGEN Biotech Co., Ltd, Beijing, China) were used for analysis of samples.

Samples of RNA subjected to RNA-seq analysis used the FastQuant RT Kit with gDNase (TIANGEN) for first-strand cDNA synthesis. Five sequences were randomly selected from the differentially expressed gene data obtained by RNA sequencing, and quantitative PCR primers were designed using NCBI primer-blast. Primer information is shown in Table 2. Primer synthesis was completed by Beijing Qingke Biotechnology Co., Ltd. The Actin gene, which was stably expressed in all RNA-seq samples and was highly expressed, was selected as the reference gene (Li 2018). The real-time PCR test uses SuperReal PreMix Plus (SYBR Green). The reaction system consisted of 20 □L, including 1□g of cDNA template (100ng / □L), and 0.75□L for each of the front and back primers. Data analysis was performed using QuantStudio ™ Design & Analysis Software (version 1.5.1, Thermo Fisher Scientific). For qRT-PCR data, relative expression $\log_2$FC was calculated using the □□Ct method, and compared with RNA sequencing data. Each sample had three replicates.

Statistical analysis

bioRxiv preprint doi: https://doi.org/10.1101/2020.07.13.198457; this version posted August 3, 2020. The copyright holder for this preprint (which was not certified by peer review) is the author/funder, who has granted bioRxiv a license to display the preprint in perpetuity. It is made available under aCC-BY-NC-ND 4.0 International license.

The diameters of *C. fructicola* strains from Shaoyang population and Wuzhishan population were counted after 96 hours of cultivation, and the average diameter of the *C. fructicola* from two populations was calculated using IBM SPSS Statistics 20 (IBM, U.S.A). The diameter of *C. fructicola* from two populations were compared by independent sample t-test and two-sided test ($\alpha = 0.05$).

Results

Comparison of Mycelia Pathogenicity of Two Populations

Diameter of lesions following inoculation was counted and results are shown in Figure 1. Average diameter of lesions following incubation with the Shaoyang population was 0.37 cm, and for the Wuzhishan population was 0.56 cm. An independent sample T test was performed on lesion diameter among the two populations, and differences were significant ($P=0.046 <0.05$).

Comparison of pathogenicity within populations and selection of representative strains

In order to select a representative strain from each of the two populations for transcriptome analysis, a comparative test of pathogenicity among the strains in the two populations was performed.

Results of the pathogenicity test of Wuzhishan populations are shown in Figure 2A. After 96 hours of inoculation, average diameter of lesions caused by 7 strains of Wuzhishan-origin was 0.50 cm (The dotted line in figure 2A). Among the seven strains tested, WZS0202b was the weakest pathogen, whereas WZS0402a and WZS0203b had the highest pathogenicity.

Results of the pathogenicity test of Shaoyang populations are shown in Figure 2B. After 96 hours of inoculation average diameter of lesions was 0.45cm (The dotted line in figure 2B). The pathogenicity of the strain SY0104b was the highest, while pathogenicity of SY0201a was the weakest.

Based on results of the two strains of *C. fructicola,* WZS0402a and SY0104b were selected for RNA sequencing.

Real-time PCR

To verify reliability of sequencing data, five differentially expressed genes were randomly selected for real-time PCR. The gene Actin was selected as the reference gene. Quantitative PCR results showed that only the gene CGGC5_435 in SY-S-vs-SY-L was significantly differentially expressed when compared to the transcriptome data.

bioRxiv preprint doi: https://doi.org/10.1101/2020.07.13.198457; this version posted August 3, 2020. The copyright holder for this preprint (which was not certified by peer review) is the author/funder, who has granted bioRxiv a license to display the preprint in perpetuity. It is made available under aCC-BY-NC-ND 4.0 International license.

All other results of gene quantification were consistent with changes observed in the transcriptome sequencing results (Figure 3). In addition, relative expression levels (log_2FC value) were not significantly different from those of the RNA sequencing results, indicating that transcriptomic sequencing results are reliable.

Statistics of differentially expressed genes

Differentially expressed genes were screened using FDR(False Discovery Rate)≤0.05 and | log_2FC | ≥1 as thresholds, and then genes were manually eliminated if they had low expression levels (FPKM <0.5), resulting in selection of WZS-S-vs-WZS-L, SY-S-vs-SY-L. Using homologous spore samples as a control, the number of genes up- and down-regulated in the infection groups were tabulated (Figure 4A). In the WZS-S-vs-WZS-L group, a total of 7846 differential genes were screened, 5951 of which expression was up-regulated (75.85%), and 1895 (24.15%) down-regulated. In the SY-S-vs-SY-L group screening, a total of 7682 differential genes were identified, 5280 (68.73%) of which were up-regulated, and 2402 (31.27%) were down-regulated. During the interaction stage of oil tea infected with *C. fructicola*, the number of up-regulated genes was significantly higher than that of down-regulated genes in the two representative strains. The number of up-regulated genes of *C. fructicola* from Wuzhishan after infection was higher than that from the Shaoyang strains. Comparison of differentially expressed gene lists post-inoculation demonstrated that 4089 genes were up-regulated in both strains after 96 hours of infection (Figure 4B). Overall, similarly expressed genes accounted for 68.7% (WZS) and 77.4% (SY) of up-regulated genes, respectively.

Gene Ontology enrichment analysis

Gene ontology (GO) function enrichment analysis was performed on differentially expressed genes following infection of WZS-S-vs-WZS-L and SY-S-vs-SY-L groups. As shown in Table 3, GO terms were screened with Pvalue ≤ 0.01 as the threshold. It was found that inoculation with the representative strain of Wuzhishan resulted in enrichment of preribosome, large ribosomal subunit and organelle ribosome GO terms. Identified molecular functions were mainly related to structural molecular activity, translation factor activity (RNA binding), and galactosidase activity. Biological processes were mainly related to the glutamine family amino acid metabolism process.

Screening of GO enrichment results of the Shaoyang group, demonstrated that enriched cell composition terms were related to ribosome precursors, large ribosome subunits, and organelle ribosomes. Molecular functions were mainly related to structural molecular activity and galactosidase activity. Identified biological processes were

bioRxiv preprint doi: https://doi.org/10.1101/2020.07.13.198457; this version posted August 3, 2020. The copyright holder for this preprint (which was not certified by peer review) is the author/funder, who has granted bioRxiv a license to display the preprint in perpetuity. It is made available under aCC-BY-NC-ND 4.0 International license.

mainly related to amino acid metabolic processes and glycoprotein metabolic processes of the glutamine family.

As presented in Table 3, it can be seen that cell composition terms for the two groups were significantly enriched in ribosomal-related annotations, but the number of differentially expressed genes in the corresponding GO annotations in the Shaoyang group was significantly lesser than that in the Wuzhishan group. Enriched molecular functions among the two groups were related to structural molecular activity and galactosidase activity, however RNA-bound translation factor activity that was enriched in the Wuzhishan group was not significantly enriched in the Shaoyang group. Enriched GO biological processes in both groups were related to glutamine amide family amino acid metabolism. However, glycoprotein metabolism was enriched in the Shaoyang group and not in the Wuzhishan group. Of the two co-enriched annotations, genes associated with galactosidase activity and amino acid metabolism of the glutamine family were most similar.

KEGG pathway enrichment analysis

Analysis of gene lists identified 7 KEGG pathways (Q value ≤0.01) following innoculation with the Wuzhishan and Shaoyang populations (Table 4). Of identified GO pathways, ribosome (ko03010), arginine and proline metabolism (ko00330) were significantly enriched in both groups, indicating that arginine and proline metabolism play an important role in processes of infection of *C. fructicola*. KEGG pathways significantly enriched only in the Wuzhishan population included ribosome biogenesis in eukaryotes (ko03008), spliceosome (ko03040), RNA transport (ko03013), RNA polymerase (ko03020), and purine metabolism (ko00230). Pathways that were significantly enriched only in the Shaoyang group included phenylalanine metabolism and beta-alanine metabolism.

Comparison of differential genes associated with the purine metabolism pathway revealed that 35 differential genes were up-regulated in the Wuzhishan group and Shaoyang group, while the remaining 27 up-regulated genes in the Wuzhishan group were not up-regulated in the Shaoyang group. Figure 5 shown the heatmap of the 27 up-regulated genes specific to the WZS group. Of up-regulated genes specific to the purine metabolism pathway following inoculation with the Wuzhishan population, 12 of the 27 genes are involved in the regulation of purine biosynthesis and catabolic metabolism (Table 5). Related downstream products of this pathway include guanylate synthase, adenylate deaminase, inosine cyclic hydrolase, and adenine phosphoribosyltransferase. The remaining 17 genes of the Wuzhishan population an up-regulated gene list is involved in RNA and DNA synthesis. Purine biosynthesis includes de novo synthesis and remedy pathway (Figure 6).

bioRxiv preprint doi: https://doi.org/10.1101/2020.07.13.198457; this version posted August 3, 2020. The copyright holder for this preprint (which was not certified by peer review) is the author/funder, who has granted bioRxiv a license to display the preprint in perpetuity. It is made available under aCC-BY-NC-ND 4.0 International license.

Discussion

C. fructicola collected in Wuzhishan have a stronger ability to infect Oil tea leaf tissue.

The two regions selected for comparison of *C. fructicola* populations are approximately 7 ° in latitude apart. Average annual rainfall of Wuzhishan is higher than that of Shaoyang, as is temperature. However, Shaoyang experiences greater temperature variation, with winter temperatures which are not suitable for proliferation of *C. fructicola* Therefore, we speculate that the anthracnose pathogen's wintering time in Wuzhishan is shorter, and that time of onset is earlier. Therefore, due to the presences of conditions which promote growth of anthracnose, we speculate that annual incidence of anthracnose in *Oil tea* in Wuzhishan is greater and occurs over longer durations of time.

A comparison of biological characteristics and pathogenicity of the two geographical populations of *C. fructicola* found that the number of lesions after 96 hours of inoculation did not differ statistically. However, there was a significant difference in the diameter of the lesions among the two populations of *C. fructicola* after inoculation with *Oil tea* for 96 hours. The spread of lesions on *Oil tea* caused by the Wuzhishan population was more serious, indicating that *C. fructicola* from Wuzhishan had a stronger ability to destroy *Oil tea* leaf tissue.

Based on results of the phenotypic experiments, the two populations of *C. fructicola* had similar abilities to infect the host however their ability to further propagate differed.

Changes in C. fructicola carbon source utilization on Oil tea leaf tissues in the late infection stage

RNA sequencing results demonstrated gene, GO term and KEGG pathway enrichment of pathways related to ribosomal activity for both populations. Enriched GO cell composition terms included organelle ribosomes in both populations, this result indicates that mitochondria and endoplasmic reticulum ribosomes might play important roles in propagation of infection and illustrates the active regulation of various proteins by pathogenic fungi after infection. Proteins like hexose transporters can be used to absorb nutrients from host cell tissues or to resist defensive immune stress in plants.

After infection by pathogenic fungi, carbohydrates in the apoplast are important carbon sources of pathogenic fungi. Previous work has found that four hexose transporters (CgHxt1, CgHxt2, CgHxt3, and CgHxt5) of *Colletotrichum graminicola* can transport a variety of hexoses, including fructose, mannose, galactose and xylose. The transporters *CgHxt2* and *CgHxt5* are only expressed in the vegetative phase based on dead plant tissue (Lingner et al. 2011). Another study showed that *MFS1* gene knockouts of *Colletotrichum lindemuthianum* had

bioRxiv preprint doi: https://doi.org/10.1101/2020.07.13.198457; this version posted August 3, 2020. The copyright holder for this preprint (which was not certified by peer review) is the author/funder, who has granted bioRxiv a license to display the preprint in perpetuity. It is made available under aCC-BY-NC-ND 4.0 International license.

defects in the use of glucose, mannose and fructose. Furthermore, semi-quantitative PCR analysis found that the *MFS1* gene was only up-regulated during the vegetative phase based on dead plant tissue 96 hours after infecting the host (Pereira et al. 2013). In the current study, GO functional enrichment analysis suggests that *C. fructicola* transforms and utilizes sugar derived from plants. Galactosidase is a class of enzymes that hydrolyze galactosyl bond-containing substances, and hydrolysis produces substances such as galactose, glucose and fructose (Yan et al. 2017). Although few enzymes related studies related to molecular mechanisms of phytopathogenic fungi exist, we suggest that galactosides were hydrolyzed by *C. fructicola* 96 hours after infection with oil tea as a new carbon source.

Glutamine family amino acids help C. fructicola resist host immune responses during late stages of infection

Glutamine family amino acids include arginine, proline, glutamic acid, and glutamine, where arginine is a precursor of proline and glutamic acid. A number of studies have demonstrated that synthesis of arginine by fungi has important effects on growth and development, production of conidia, *MoARG1*, *MoARG5*, *6* and *MoARG7* by *Magnaporthe oryzae* (Zhang et al. 2015), *ARG1* by *Fusarium oxysporum* (Namiki et al. 2001), *PATH-19* and *PATH-35* oby *Colletotrichum higginsianum* (Takahara et al. 2012). The anti-stress effects of proline in plants and endophytic fungi has been widely studied. A number of plants can accumulate large amounts of proline when exposed to stresses such as reactive oxygen stress, therefore proline is often used as a physiological or biochemical indicators of plant stress resistance (Zhu et al. 2009). However, the role of proline in pathogenic fungi has not received much attention. For example, proline has been reported to remove reactive oxygen species in *Colletotrichum truncatum* (Chen C, et al, 2005).

Glutamine and glutamic acid can be interconverted by enzymes: In *Saccharomyces cerevisiae*, glutamine can be directly converted to glutamate by glutamine enzymes. In addition, glutamine can be degraded or converted to glutamate by NADH-dependent glutamate synthase (Miller and Magasanik 1990). In addition, glutamine and glutamic acid are involved in biosynthesis of glutathione. Glutathione exists in two forms: an oxidized state (GSSG) or reduced state (GSH). During conversion of GSH to GSSG, its thiol group is used as an electron donor to maintain the activity of thiol proteins and enzymes, and to reduce host-derived ROS stress on pathogen cells. Furthermore, the glutathione antioxidant system is important to pathogens to facilitate infection of hosts, therefore glutamine family amino acids play an important role in resisting plant immune responses.

Up-regulation of purine metabolism improves growth of C. fructicola

bioRxiv preprint doi: https://doi.org/10.1101/2020.07.13.198457; this version posted August 3, 2020. The copyright holder for this preprint (which was not certified by peer review) is the author/funder, who has granted bioRxiv a license to display the preprint in perpetuity. It is made available under aCC-BY-NC-ND 4.0 International license.

By use of GO analysis, it was observed that ribosome-related genes of Wuzhishan and Shaoyang fungi populations were significantly up-regulated following infection. However, the number of differentially expressed genes associated with ribosome-related annotations in the Shaoyang group was significantly less than that in the Wuzhishan group. In addition, comparison of GO analysis results of differentially expressed gene lists demonstrated enrichment in activity of translation factors for the Wuzhishan group but not the Shaoyang group, indicating that the translation factor activity of the Wuzhishan group was significantly higher during the process of ribosomal translation. KEGG enrichment analysis indicated that the Wuzhishan group was significantly enriched in signal pathways such as spliceosome, RNA transport, and RNA polymerase, while they were not significantly enriched in the Shaoyang group. Differences in transcriptional and translational activity of the two populations of *C. fructicola* indicate that the Wuzhishan population are most active, and that enriched pathways and differentially expressed genes might be related to its stronger pathogenicity.

Purine nucleotide metabolism is necessary for biological metabolic processes and expression of genetic information, and supports a number of physiological and biochemical reactions (Zrenner et al. 2006). Purine in living organisms can be divided into adenine, guanine, xanthine and hypoxanthine according to their base pairs. Purines are not only an important part of nucleic acid, but also participate in protein translation, phosphate utilization and energy metabolism (Gauthier et al. 2008). Using KEGG enrichment analysis, we found that differentially expressed genes in the Wuzhishan group were significantly enriched in processes related to purine metabolism, indicating that *C. fructicola* in Wuzhishan group induce purine related genes associated with the nucleotide metabolic pathway after infection. We found that 33 differentially expressed genes in the Wuzhishan group and Shaoyang group were up-regulated following infection, while the remaining 29 of the 62 up-regulated genes were specific to the Wuzhishan group. There were no significant differences in expression levels before and after infection. Twelve of the 29 genes that were specific to the Wuzhishan group were involved in regulation of purine biosynthesis and catabolic metabolism (Table 5), especially biosynthetic pathways. Of the 12 genes, four (*PRS5*, *ADE3*, *ADE17*, *ADE6*) are involved in regulating biosynthesis of IMP in the purine de novo synthesis pathway, three (*ADSS*, *ADK*, *GUA1*) are involved in regulating ATP and GTP synthesis by IMP, one (*APT1*) participates in regulation of purine rescue pathways, and four (*AAH1*, *ADA1*, *UAZ*, *NT5E*) participate in regulation of purine degradation pathways.

Genes that were specifically up-regulated in the Wuzhishan group play important roles in purine anabolic metabolism, and data show that the purine de novo synthesis pathway is directly related to the growth and development and pathogenicity of pathogenic fungi. Previously, it has been observed that the guanylate kinase

bioRxiv preprint doi: https://doi.org/10.1101/2020.07.13.198457; this version posted August 3, 2020. The copyright holder for this preprint (which was not certified by peer review) is the author/funder, who has granted bioRxiv a license to display the preprint in perpetuity. It is made available under aCC-BY-NC-ND 4.0 International license.

and inosine-5'-phosphate lactate dehydrogenase (IMPDH) play key roles in the GTP synthesis pathway. Knock down of the Guanylate kinase gene, *MoGuk2*, in *Magnaporthe oryzae* led to reductions in the expansion of hyphae by the host (Cai et al. 2017). The five active sites of the IMPDH coding gene, *MoIMD4,* are involved in regulating the pathogenicity of *M. oryzae*, thus *MoIMD4* knockout mutant are more susceptible to infection than wild-type rice (Yang et al. 2019). *ACD1* of *Fusarium graminearum* participates in the regulation of the conversion process of AMP to IMP. The knockout mutant of *ACD1* cannot form ascospores, and the expansion ability of the infection hyphae decreases in the host cells. Further analyses of phenotypes were performed in the knockout mutant of the *APT1*, *XPT1*, *AAH1*, and *GUD1* genes, revealed that the growth rate and pathogenicity of these four mutants were not significantly different from those of the wild type, which indicated when a de novo purine synthesis pathway exist in *F. graminearum*, the *APT1*, *XPT1*, *AAH1*, and *GUD1* genes involved in regulating the purine salvage pathway are not necessary for the growth and pathogenicity of *F. graminearum*. (Sun 2019). Our analysis indicates that representative strains of Wuzhishan *C. fructicola* have greater on purine metabolism, which might be related to its greater pathogenicity.

Acknowledgement

We thank the sub-project (Ecological Adaptability and Molecular Basis of the Spread of *Camellia oleifera* Anthracnose) of the National Key R & D Project (2017YFD0600103-3) and Graduate Research Project of Central South University of Forestry and Technology (No. 20181010) for financial support.

References

Cai X, Zhang X, Li X, Liu M, Liu X, Wang X, Zhang H, Zheng X, Zhang Z (2017) The Atypical Guanylate Kinase MoGuk2 Plays Important Roles in Asexual/Sexual Development, Conidial Septation, and Pathogenicity in the Rice Blast Fungus. Front Microbiol 8(2467-2467 doi:10.3389/fmicb.2017.02467

Chen C, Xia R, Chen H, He Y (2018) TBtools, a Toolkit for Biologists integrating various biological data handling tools with a user-friendly interface. BioRxiv:289660

Chen, C., & Dickman, M. B. (2005). Proline suppresses apoptosis in the fungal pathogen Colletotrichum trifolii. *Proceedings of the National Academy of Sciences of the United States of America, 102(9)*, pp. 3459-3464. doi:10.1073/pnas.0407960102

Chen X-M, Wang J, Sun S, Wu H-X (2009) Histopathological observation on the invasion of Colletotrichum gloeosporioidesto oil tea. Forest Pest and Disease 28(5):6-9

bioRxiv preprint doi: https://doi.org/10.1101/2020.07.13.198457; this version posted August 3, 2020. The copyright holder for this preprint (which was not certified by peer review) is the author/funder, who has granted bioRxiv a license to display the preprint in perpetuity. It is made available under aCC-BY-NC-ND 4.0 International license.

323 Cui X, Wang W, Yang X, Li S, Qin S, Rong J (2016) Potential distribution of wild Camellia oleifera based on
324 ecological niche modeling. Biodiversity Science 24(10):1117-1128 doi:10.17520/biods.2016164
325 Curry KJ, Abril M, Avant JB, Smith BJ (2002) Strawberry Anthracnose: Histopathology of Colletotrichum
326 acutatum and C. fragariae. Phytopathology® 92(10):1055-1063 doi:10.1094/phyto.2002.92.10.1055
327 Deng L, Liu J, Zhou G (2017) Antifungal activity of broth of Camellia anthracnose of antagonistic actinomycete
328 CF17 and isolation and purification of its antifungal substances. Journal of Fujian Agriculture and Forestry
329 University (Natural Science Edition) 46(1):15-20
330 Deng YZ, Naqvi NI (2019) Metabolic Basis of Pathogenesis and Host Adaptation in Rice Blast. Annu Rev
331 Microbiol 73(1):601-619 doi:10.1146/annurev-micro-020518-115810
332 Gauthier S, Coulpier F, Jourdren L, Merle M, Beck S, Konrad M, Daignan-Fornier B, Pinson B (2008) Co-
333 regulation of yeast purine and phosphate pathways in response to adenylic nucleotide variations. Molecular
334 Microbiology 68(6):1583-1594 doi:10.1111/j.1365-2958.2008.06261.x
335 Jiang SQ, Li H (2018) First Report of Leaf Anthracnose Caused by Colletotrichum karstii on Tea-Oil Trees
336 (Camellia oleifera) in China. Plant Dis 102(3):674 doi:10.1094/pdis-08-17-1195-pdn
337 Li H (2018) Population Genetic Analyses of the Fungal Pathogen Colletotrichum on Tea-Oil Trees in China and
338 Characterization of a MAPK gene CfPMK1 in the Pathogen. Central South University of Forestry &
339 Technology
340 Li H, Li Y, Jiang S (2017) Pathogen of Oil-Tea Trees Anthracnose Caused by Colletotrichum spp. in Hunan
341 Province. Scientia Silvae Sinicae 53(8):43-53
342 Li H, Zhou G-Y, Liu J-A, Xu J (2016) Population Genetic Analyses of the Fungal Pathogen Colletotrichum
343 fructicola on Tea-Oil Trees in China. PLoS ONE 11(6):e0156841-e0156841
344 doi:10.1371/journal.pone.0156841
345 Lingner U, Münch S, Deising HB, Sauer N (2011) Hexose transporters of a hemibiotrophic plant pathogen:
346 functional variations and regulatory differences at different stages of infection. The Journal of biological
347 chemistry 286(23):20913-20922 doi:10.1074/jbc.M110.213678
348 Ma W (2010) The evaluation for forests ecosystem purify the atmosphere function in Shaoyang city. Journal of
349 Central South University of Forestry & Technology 30(02):51-54
350 Miller SM, Magasanik B (1990) Role of NAD-linked glutamate dehydrogenase in nitrogen metabolism in
351 Saccharomyces cerevisiae. Journal of bacteriology 172(9):4927-4935 doi:10.1128/jb.172.9.4927-4935.1990
352 Morrow CA, Valkov E, Stamp A, Chow EWL, Lee IR, Wronski A, Williams SJ, Hill JM, Djordjevic JT, Kappler

bioRxiv preprint doi: https://doi.org/10.1101/2020.07.13.198457; this version posted August 3, 2020. The copyright holder for this preprint (which was not certified by peer review) is the author/funder, who has granted bioRxiv a license to display the preprint in perpetuity. It is made available under aCC-BY-NC-ND 4.0 International license.

353 U, Kobe B, Fraser JA (2012) De novo GTP biosynthesis is critical for virulence of the fungal pathogen
354 Cryptococcus neoformans. PLoS pathogens 8(10):e1002957-e1002957 doi:10.1371/journal.ppat.1002957
355 Namiki F, Matsunaga M, Okuda M, Inoue I, Nishi K, Fujita Y, Tsuge T (2001) Mutation of an Arginine
356 Biosynthesis Gene Causes Reduced Pathogenicity in Fusarium oxysporum f. sp. melonis. Molecular Plant-
357 Microbe Interactions® 14(4):580-584 doi:10.1094/mpmi.2001.14.4.580
358 Pereira MF, De Araújo Dos Santos CM, De Araújo EF, De Queiroz MV, Bazzolli DMS (2013) Beginning to
359 understand the role of sugar carriers in Colletotrichum lindemuthianum: the function of the gene mfs1.
360 Journal of Microbiology 51(1):70-81 doi:10.1007/s12275-013-2393-5
361 Su F (2018) Study on Germplasm Resources and Antioxidant Activity of Wild Tea Trees in Wuzhishan City.
362 Hainan University
363 Sun M (2019) Characterization of mRNA Splicing Related SNU66 and Purine Nucleotide Metabolism Pathway
364 Genes in Fusarium Graminearum. Northwest A & F University
365 Takahara H, Huser A, O'connell R (2012) Two arginine biosynthesis genes are essential for pathogenicity of
366 Colletotrichum higginsianum on Arabidopsis. Mycology 3(1):54-64
367 Tang YL, Zhou GY, Li H (2015) Identification of a New Anthracnose of Camellia oleifera Based on Multiple-
368 gene Phylogeny. Chinese Journal of Tropical crops 36(5):972-977
369 Wang H, Lin F, Wang Z (2004) Mechanical Penetrating Force of Appressoria of Plant Pathogenic Fungi
370 Mycosystema 23(1):151-157
371 Yan QJ, Liu Y, Jiang ZQ (2017) Advances in Microbial α-Galactosidase. Journal of Microbiology 37(03):1-9
372 Yang L, Ru Y, Cai X, Yin Z, Liu X, Xiao Y, Zhang H, Zheng X, Wang P, Zhang Z (2019) MoImd4 mediates
373 crosstalk between MoPdeH-cAMP signalling and purine metabolism to govern growth and pathogenicity in
374 Magnaporthe oryzae. Molecular plant pathology 20(4):500-518 doi:10.1111/mpp.12770
375 Ye J, He W (2011) Forest pathology. China Forestry Press, Beijing
376 Zhang Y, Shi H, Liang S, Ning G, Xu N, Lu J, Liu X, Lin F (2015) MoARG1, MoARG5,6 and MoARG7 involved
377 in arginine biosynthesis are essential for growth, conidiogenesis, sexual reproduction, and pathogenicity in
378 Magnaporthe oryzae. Microbiological Research 180(11-22 doi:10.1016/j.micres.2015.07.002
379 Zheng DJ, Pan XZ, Zhang DM (2016) Survey and Analysis on Tea-oil Camellia Resource in Hainan. Journal of
380 Northwest Forestry University 31(1):130-135
381 Zhou W, Wen Q, Yang J, Wang J, Xu L, Xu L (2017) Establishment of DNA fingerprints and cluster analysis for
382 oil camellia cultivars based on SSR markers. Fenzi ZhiwuYuzhong (Molecular Plant Breeding) 15(1):238-

bioRxiv preprint doi: https://doi.org/10.1101/2020.07.13.198457; this version posted August 3, 2020. The copyright holder for this preprint (which was not certified by peer review) is the author/funder, who has granted bioRxiv a license to display the preprint in perpetuity. It is made available under aCC-BY-NC-ND 4.0 International license.

383 249

384 Zhou Y (2015) Mechanisms of interaction between Pichia membranaceus-bound chitosan and anthrax-citrus fruits.
385 Chinese Society of Plant Pathology:201-202

386 Zhu H, Wang W, Yan Y (2009) Effect of proline on plant growth under different stress conditions. Journal of
387 Northeast Forestry University 37(4):86-89

388 Zrenner R, Stitt M, Sonnewald U, Boldt R (2006) PYRIMIDINE AND PURINE BIOSYNTHESIS AND
389 DEGRADATION IN PLANTS. Annual Review of Plant Biology 57(1):805-836
390 doi:10.1146/annurev.arplant.57.032905.105421

391

392

393 **Tables**

394 Table 1 Geographical and climatic features of Wuzhishan and Shaoyang

Items	Hainan Wuzhishan	Hunan Shaoyang
latitude and longitude	East longitude 109°19′~109°44′ North latitude 18°38′~19°02′	East longitude 109°49'~112°57' North latitude 25°58'~27°40'
Climate type	Tropical ocean monsoon climate	Subtropical monsoon humid climate
Average annual temperature	22.4°C	15°C ~22°C
The highest temperature in history (1959-2019)	35.9°C	38°C
The lowest temperature in history (1959-2019)	11°C	-22°C
Average annual rainfall	2444mm	1368mm
Climate diversity	Large temperature difference between day and night; high temperatures throughout the year; Heavy rainfall in summer and extremely short spring and autumn.	Mild climate, distinct four seasons, large seasonal temperature difference; sufficient rainfall, heavy rain in spring and summer; often dry in summer and autumn

395

396 Table 2 Primer related information for real-time PCR

Gene ID	Primer Sequence (5’→3’)	Tm
CGGC5_1052	F: GCTCAACCGCTTCCTGTCC R: GTTGAGGCTCTGCATGTTGG	60

MSTRG.12379	F: ATCCCAGCCAGTGGTCAAAG R: GACCTCAACACCGACTCCAG	60
CGGC5_14884	F: GAATCCCCAGGCACCTTTCA R: TTGAGCAGGATGCGAGAGC	60
CGGC5_8685	F: ACCTCAGGGCAACAACAACA R: AGGCTGTGGGAGTAGTAGGG	60
CGGC5_435	F: ACTTCCATCGTCTGGCAAGG R: ATAGGGCGCCGATGAAAGAG	60
Actin	F: ATGTGCAAGGCCGGTTTCGC R: TACGAGTCCTTCTGGCCCAT	60

397

398 Table 3 GO terms significantly enriched in oil tea leaves inoculated with strains of C. fructicola and related up-regulated genes

GO ID	Term	All genes with GO annotation	DEGs with GO annotation		Pvalue	
			WZS	SY	WZS	SY
GO:0030684	preribosome	88	84	58	6.17E-26	1.42E-07
GO:0015934	large ribosomal subunit	38	37	28	9.39E-13	1.08E-05
GO:0000313	organellar ribosome	48	44	36	2.61E-12	2.71E-07
GO:0005198	structural molecule activity	61	49	37	1.36E-10	8.63E-05
GO:0008135	translation factor activity, RNA binding	65	42	23	5.36E-05	0.6050

GO:0015925	galactosidase activity	20	16	15	3.25E-04	4.76E-04
GO:0009064	glutamine family amino acid metabolic process	51	32	31	1.55E-03	5.61E-04
GO:0009100	glycoprotein metabolic process	30	11	18	0.7554	9.73E-03

399

400 Table 4 KEGG pathways significantly enriched in oil tea leaves inoculated with strains of C. fructicola and related up-regulated genes

Pathway ID	Pathway	All genes with pathway annotation	DEGs with pathway annotation		Qvalue	
			WZS	SY	WZS	SY
ko03010	Ribosome	102	99	88	7.04E-30	2.34E-20
ko00330	Arginine and proline metabolism	79	51	50	3.45E-03	1.07E-03
ko00230	Purine metabolism	99	62	37	3.10E-03	0.9999
ko03008	Ribosome biogenesis in eukaryotes	71	56	42	9.59E-08	0.0231
ko03013	RNA transport	93	63	41	9.49E-05	0.9079
ko03020	RNA polymerase	26	22	12	5.79E-04	0.9727
ko03040	Spliceosome	88	68	40	1.33E-08	0.7774

401

402 Table 5 12 Up-regulated genes specific to the WZS group related to purine synthesis and catabolism

Gene ID	Gene	Description	Pathway Module
CGGC5_8860	APT1	Adenine phosphoribosyltransferase	--
CGGC5_5780	NT5E	5'-nucleotidase	--

CGGC5_5691	UAZ	Uricase	Purine degradation
CGGC5_3653	PRS5	Ribose-phosphate pyrophosphokinase	PRPP biosynthesis
CGGC5_3645	ADE6	Phosphoribosylformylglycinamidine synthase	IMP biosynthesis
CGGC5_2412	ADE17	IMP cyclohydrolase	IMP biosynthesis
CGGC5_15250	ADA1	AMP deaminase	--
CGGC5_13215	AAH1	Adenosine deaminase	--
CGGC5_11685	GUA1	GMP synthase	Guanine ribonucleotide biosynthesis
CGGC5_11516	SPCC830.11c	Adenylate kinase	Adenine ribonucleotide biosynthesis
CGGC5_11342	ADE3	Phosphoribosylformylglycinamidine synthase, partial	IMP biosynthesis
CGGC5_11063	NCU09789	Adenylosuccinate synthetase	Adenine ribonucleotide biosynthesis

403

404 **Figures**

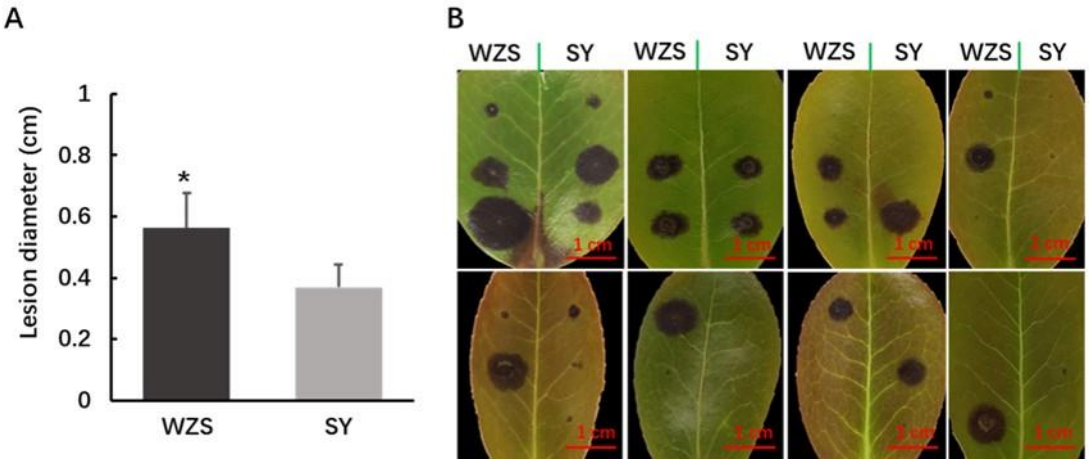

405

406 **Fig. 1** Pathogenicity of *C. fructicola* populations collected from Shaoyang and Wuzhishan to oil-tea leaves. A: Lesion diameters on oil-tea leaves following inoculation with *C.*

407 *fructicola* populations from Wuzhishan and Shaoyang. Error bars are mean ± standard deviation and asterisks represent significance at *P<0.05(P=0.046). B: Lesions after 96

408 hours of inoculation. Green vertical lines represent leaf veins. Wuzhishan strains and Shaoyang strains were inoculated on the left and right sides of leaves.

409

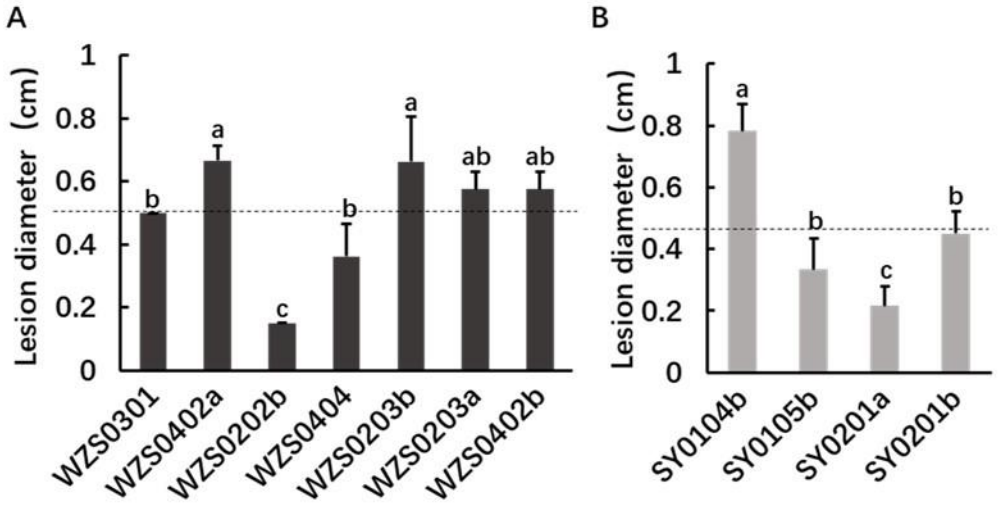

410

411 **Fig. 2** Pathogenicity of *C. fructicola* strains. A: Pathogenicity of 7 *C. fructicola* strains from Wuzhishan. The dotted line is the average lesion diameter. Error bars are mean ±

412 standard deviation. B: Pathogenicity of 4 *C. fructicola* strains from Shaoyang. The dotted line is the average lesion diameter. Error bars are mean ± standard deviation.

413

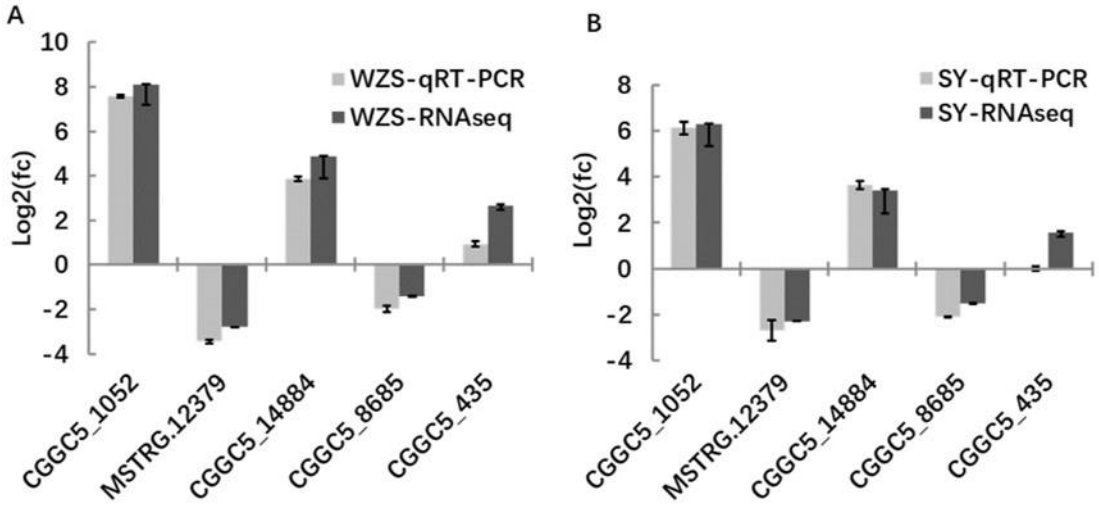

414

415 **Fig. 3** Gene expression of qRT-PCR and RNAseq. A: qRT-PCR and RNAseq verification of WZS-S-vs-WZS-L. B: qRT-PCR and RNAseq verification result of SY-S-vs-SY-

416 L.

417

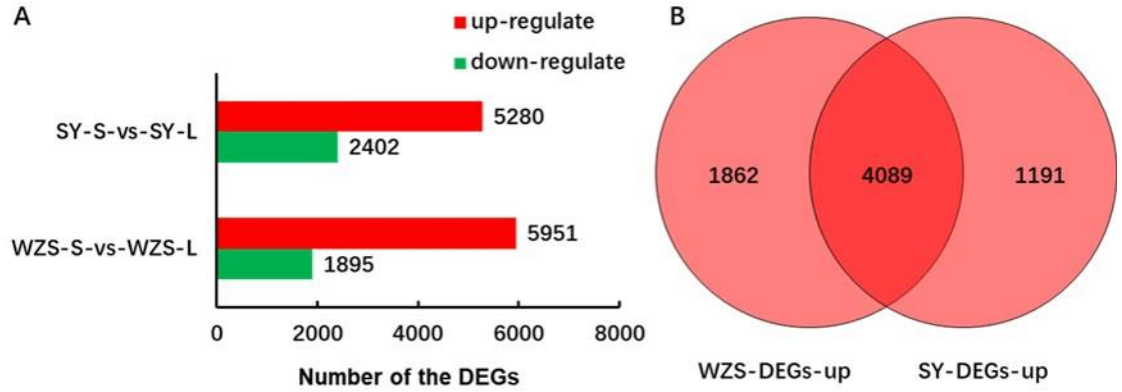

418

419 **Fig. 4** Overview of differentially expressed genes. A: Comparison of differential genes before and after infection. B: Venn diagram of number of up-regulated genes after

420 infection.

421

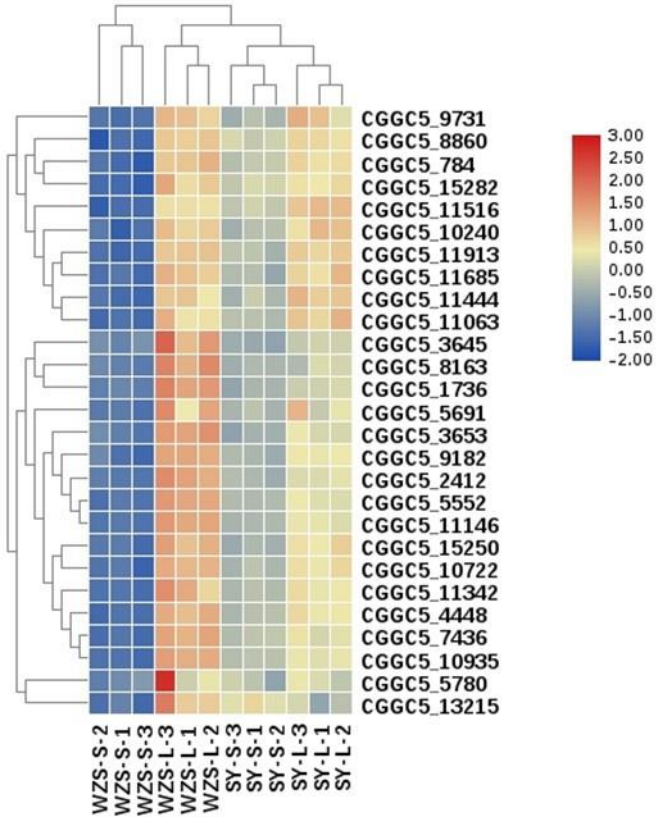

422

423 **Fig. 5** Heatmap of the 27 up-regulated genes specific to the WZS group. The heatmap was created using the TBtool (version 0.66837, (Chen et al. 2018)) function “heatmap”

424 with default parameter setting and shows normalized FPKM values.

425

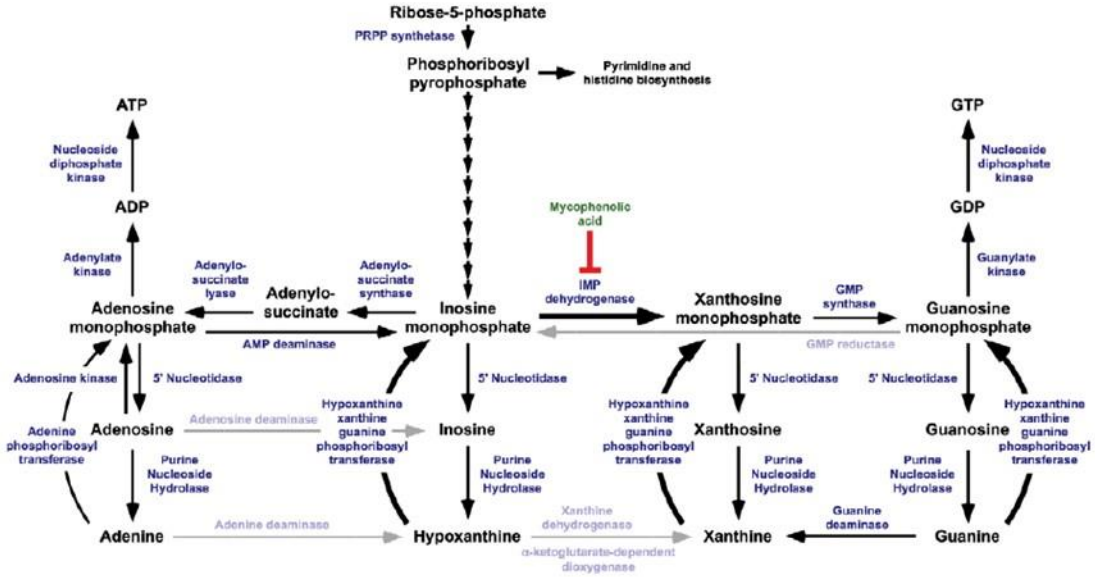

426

427 **Fig. 6** Components of the purine metabolic pathway (Morrow et al. 2012). The de novo synthesis pathway uses 5-phosphate ribose (Ribose-5P) as the raw material, and
428 generates phosphoribosyl pyrophosphate (PRPP) via phosphoribosyl pyrophosphate kinase (PRS), which then synthesizes inosinic acid (IMP) through ten consecutive reactions
429 catalyzed by various enzymes. In the de novo synthesis pathway, IMP is converted into adenylate (AMP), or to xanthosine (XMP) and then guanylate (GMP), and finally to
430 ATP and GTP. In the rescue pathway, free adenine and guanine in cells synthesize AMP and GMP under the action of adenine phosphoribosyltransferase (APT). The purine
431 degradation pathway first converts purine nucleotides, such as AMP and GMP, into xanthine by various enzymes. Xanthine is finally degraded to produce uric acid.

432

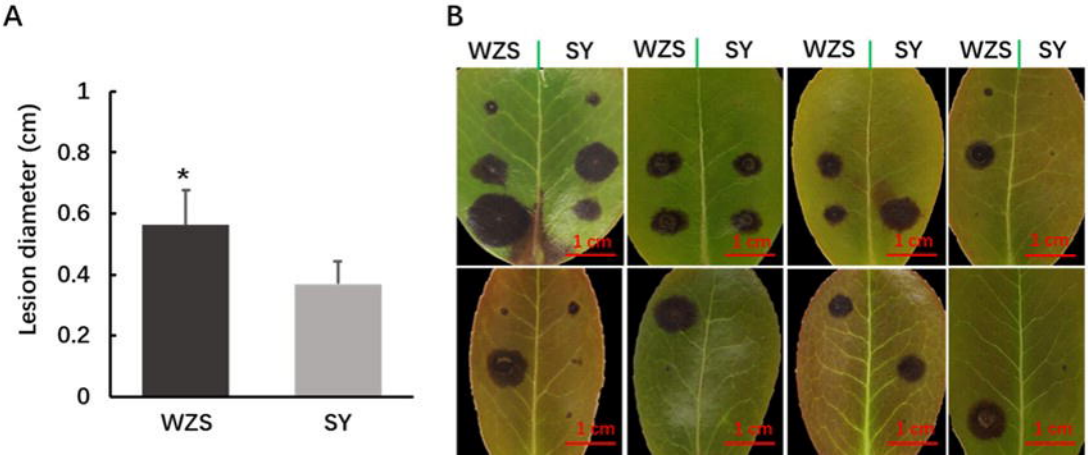
A
Lesion diameter (cm)
1
0.8
0.6
0.4
0.2
0
*
WZS
SY
B
WZS
SY
WZS
SY
WZS
SY
1 cm

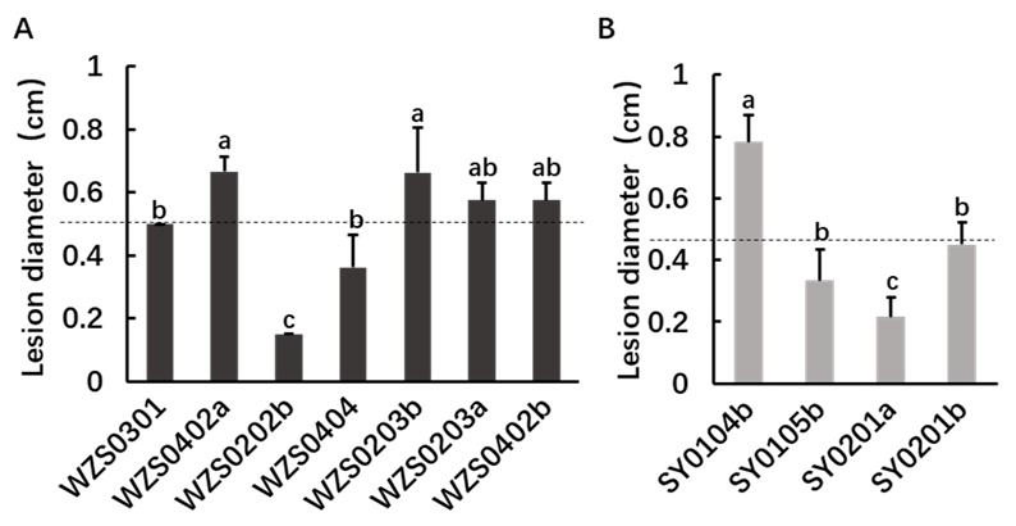
A
Lesion diameter (cm)
1
0.8
0.6
0.4
0.2
0
b
a
c
b
a
ab
ab
WZS0301
WZS0402a
WZS0202b
WZS0404
WZS0203b
WZS0203a
WZS0402b
B
Lesion diameter (cm)
1
0.8
0.6
0.4
0.2
0
a
b
c
b
SY0104b
SY0105b
SY0201a
SY0201b

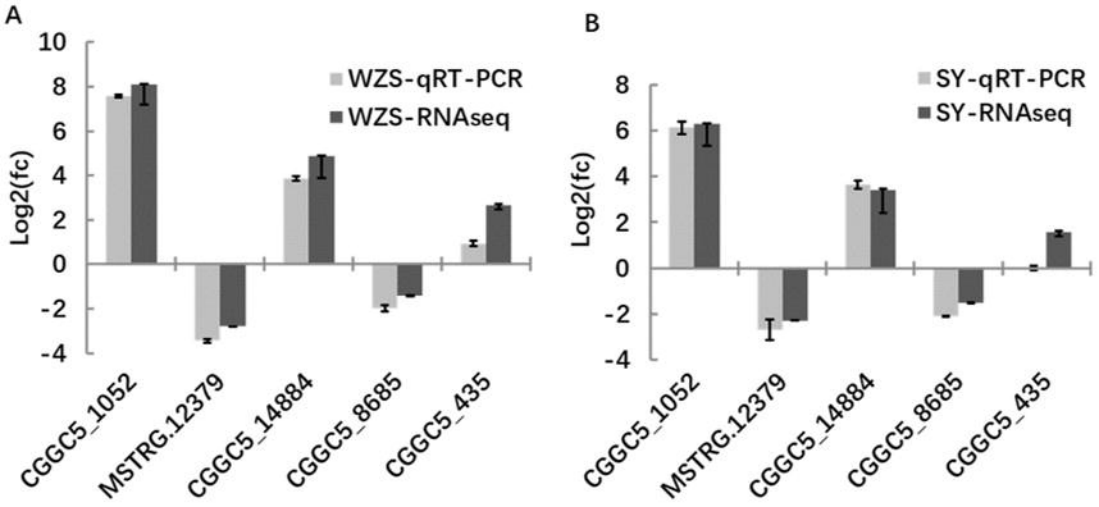
A
10
8
6
4
2
0
-2
-4
Log2(fc)
WZS-qRT-PCR
WZS-RNAseq
CGGC5_1052
MSTRG.12379
CGGC5_14884
CGGC5_8685
CGGC5_435
B
8
6
4
2
0
-2
-4
Log2(fc)
SY-qRT-PCR
SY-RNAseq
CGGC5_1052
MSTRG.12379
CGGC5_14884
CGGC5_8685
CGGC5_435

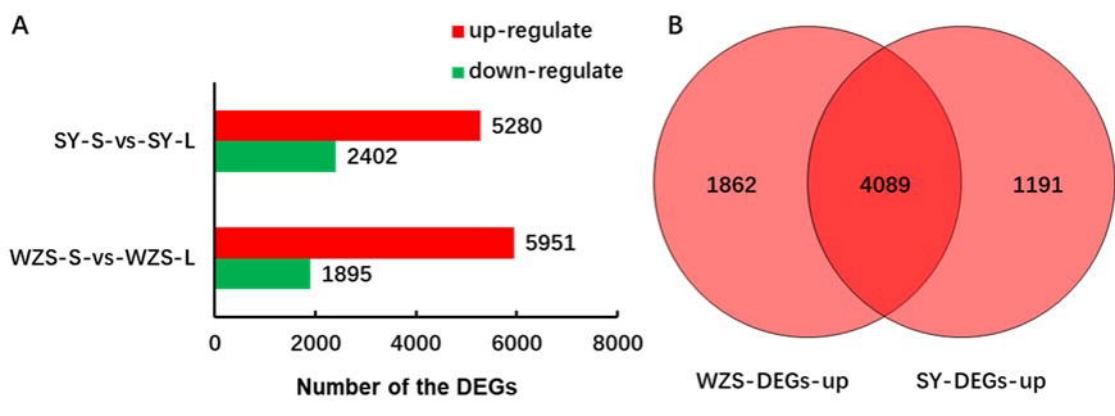
A
up-regulate
down-regulate
SY-S-vs-SY-L
5280
2402
WZS-S-vs-WZS-L
5951
1895
0
2000
4000
6000
8000
Number of the DEGs
B
1862
4089
1191
WZS-DEGs-up
SY-DEGs-up

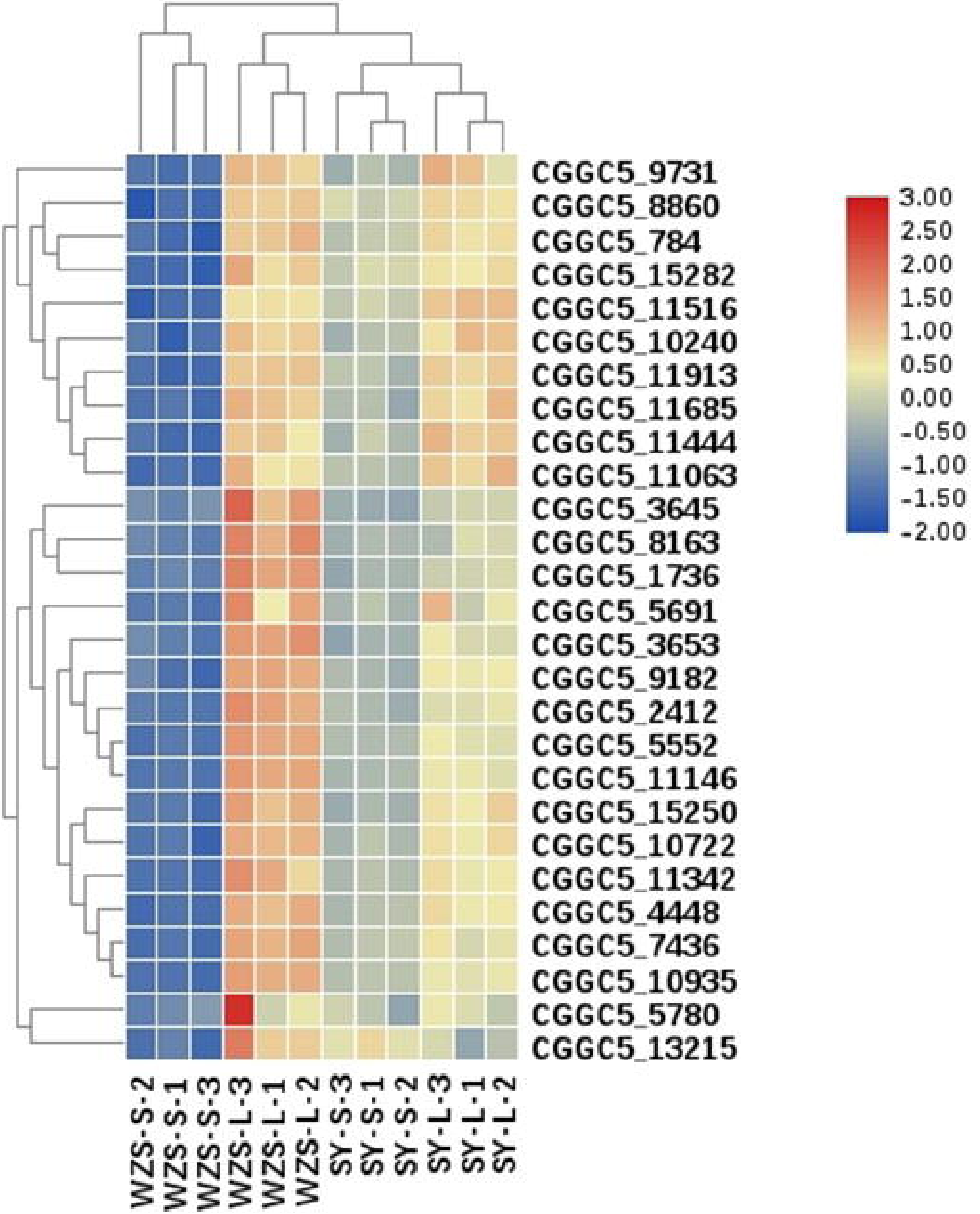
CGGC5_9731
CGGC5_8860
CGGC5_784
CGGC5_15282
CGGC5_11516
CGGC5_10240
CGGC5_11913
CGGC5_11685
CGGC5_11444
CGGC5_11063
CGGC5_3645
CGGC5_8163
CGGC5_1736
CGGC5_5691
CGGC5_3653
CGGC5_9182
CGGC5_2412
CGGC5_5552
CGGC5_11146
CGGC5_15250
CGGC5_10722
CGGC5_11342
CGGC5_4448
CGGC5_7436
CGGC5_10935
CGGC5_5780
CGGC5_13215
WZS-S-2
WZS-S-1
WZS-S-3
WZS-L-3
WZS-L-1
WZS-L-2
SY-S-3
SY-S-1
SY-S-2
SY-L-3
SY-L-1
SY-L-2
3.00
2.50
2.00
1.50
1.00
0.50
0.00
-0.50
-1.00
-1.50
-2.00

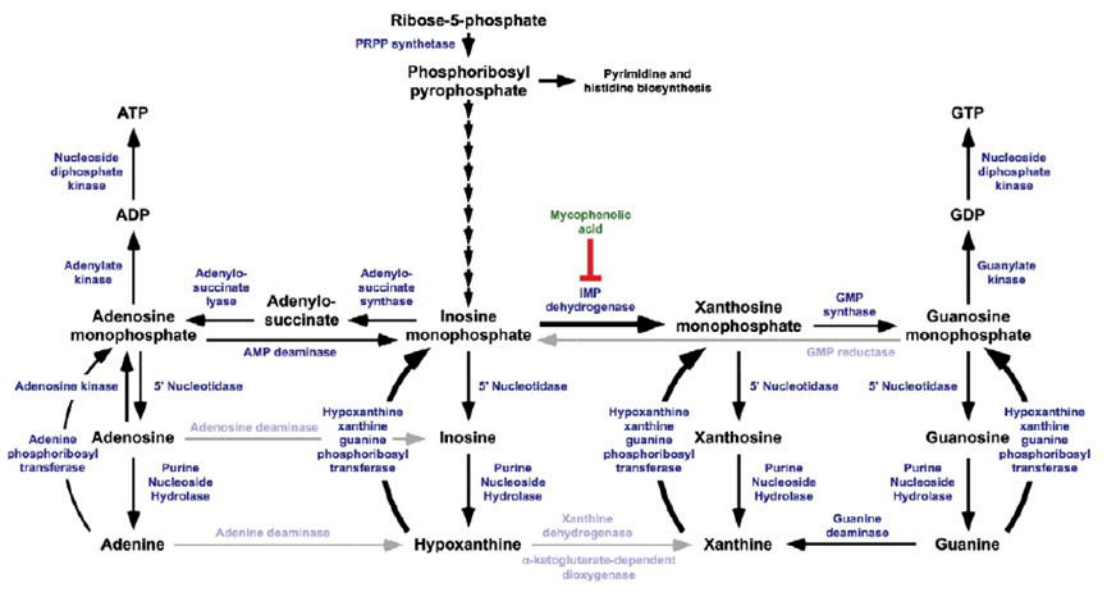
Ribose-5-phosphate
PRPP synthetase
Phosphoribosyl pyrophosphate
Pyrimidine and histidine biosynthesis
ATP
Nucleoside diphosphate kinase
ADP
Adenylate kinase
Adenosine monophosphate
Adenylo-succinate lyase
Adenylo-succinate
Adenylo-succinate synthase
AMP deaminase
Inosine monophosphate
Mycophenolic acid
IMP dehydrogenase
Xanthosine monophosphate
GMP synthase
GMP reductase
Guanosine monophosphate
GTP
Nucleoside diphosphate kinase
GDP
Guanylate kinase
Adenosine kinase
5' Nucleotidase
Adenosine
Adenosine deaminase
Hypoxanthine xanthine guanine phosphoribosyl transferase
Inosine
Xanthosine
Guanosine
Adenine phosphoribosyl transferase
Purine Nucleoside Hydrolase
Adenine
Hypoxanthine
Xanthine dehydrogenase
α-ketoglutarate-dependent dioxygenase
Xanthine
Guanine deaminase
Guanine